ATP-gated ion channels mediate adaptation to elevated sound levels

Gary D. Housley[a,b,1], Rachel Morton-Jones[b], Srdjan M. Vlajkovic[b,c], Ravindra S. Telang[b,c], Vinthiya Paramananthasivam[b], Sherif F. Tadros[a], Ann Chi Yan Wong[a], Kristina E. Froud[a], Jennie M. E. Cederholm[a], Yogeesan Sivakumaran[a], Peerawuth Snguanwongchai[a], Baljit S. Khakh[d,e], Debra A. Cockayne[f], Peter R. Thorne[b,c,g,2], and Allen F. Ryan[h,i,j,2]

[a]Department of Physiology and Translational Neuroscience Facility, School of Medical Sciences, University of New South Wales, Sydney, NSW 2052, Australia; [b]Department of Physiology, [c]Centre for Brain Research, School of Medical Sciences, and [g]Section of Audiology, School of Population Health, University of Auckland, Auckland 1142, New Zealand; Departments of [d]Physiology and [e]Neurobiology, David Geffen School of Medicine, University of California, Los Angeles, CA 90095; [f]Boston Scientific, San Jose, CA 95134; Departments of [h]Surgery and [i]Neurosciences, University of California at San Diego, Ja Jolla, CA 92037; and [j]San Diego Veterans Administration Medical Center, La Jolla, CA 92037

Edited* by Lutz Birnbaumer, National Institute of Environmental Health Sciences, Research Triangle Park, NC, and approved March 22, 2013 (received for review December 20, 2012)

The sense of hearing is remarkable for its auditory dynamic range, which spans more than 10^{12} in acoustic intensity. The mechanisms that enable the cochlea to transduce high sound levels without damage are of key interest, particularly with regard to the broad impact of industrial, military, and recreational auditory overstimulation on hearing disability. We show that ATP-gated ion channels assembled from $P2X_2$ receptor subunits in the cochlea are necessary for the development of temporary threshold shift (TTS), evident in auditory brainstem response recordings as sound levels rise. In mice null for the *P2RX2* gene (encoding the $P2X_2$ receptor subunit), sustained 85-dB noise failed to elicit the TTS that wild-type (WT) mice developed. ATP released from the tissues of the cochlear partition with elevation of sound levels likely activates the broadly distributed $P2X_2$ receptors on epithelial cells lining the endolymphatic compartment. This purinergic signaling is supported by significantly greater noise-induced suppression of distortion product otoacoustic emissions derived from outer hair cell transduction and decreased suprathreshold auditory brainstem response input/output gain in WT mice compared with *P2RX2*-null mice. At higher sound levels (≥95 dB), additional processes dominated TTS, and *P2RX2*-null mice were more vulnerable than WT mice to permanent hearing loss due to hair cell synapse disruption. *P2RX2*-null mice lacked ATP-gated conductance across the cochlear partition, including loss of ATP-gated inward current in hair cells. These data indicate that a significant component of TTS represents $P2X_2$ receptor-dependent purinergic hearing adaptation that underpins the upper physiological range of hearing.

noise-induced hearing loss | acoustic overstimulation | permanent threshold shift | auditory neurotransmission | sound transduction

Sensory systems are characterized by adaptation processes that sustain transduction as stimulus intensity increases. The mammalian auditory system operates across an acoustic power range of ~120 dB, measured on the logarithmic decibel scale. The mechanism for the extraordinary acuity of the cochlea (recalling the age-old adage of "hearing a pin drop") arises from the commitment of 75% of the sensory hair cells, the outer hair cells, to electromechanical (reverse) transduction, driving a "cochlear amplifier." The nonlinear outer hair cell reverse transduction provides an ~40-dB gain at hearing threshold, reducing to zero as sound levels rise (1). A major challenge for auditory physiology is to understand how hearing is preserved in the face of acoustic overstimulation, as noise can damage the cochlea and can greatly exacerbate hearing loss with aging (2). Given the recent propensity for direct delivery of high-level recreational sound to the ear canals by personal music players and, more broadly, the impact on our hearing of noise from industrial and military environments, there is an imperative to better understand the intrinsic mechanisms that enable the cochlea to accommodate loud sound.

Known mechanisms by which the cochlea adjusts its sensitivity to loud sound include the middle-ear muscle reflex and efferent feedback to the outer hair cells. The middle-ear muscle reflex (3) is largely driven by vocalization or intense low-frequency sound, and fatigues after a few minutes. Efferent neuronal adaptation is even more rapid (milliseconds to seconds) and provides dynamic modulation that enables the cochlea to unmask sounds of attentive interest from background noise. The olivocochlear efferent system is to some extent otoprotective against noise damage (4), and contributes to "conditioning," where sustained moderate sound exposure toughens the cochlea against subsequent acoustic overstimulation (5). However, this efferent feedback to the cochlea rapidly adapts at sound levels well below safe upper hearing limits (85 dB LAeq [equivalent continuous A-weighted sound pressure level (dB)]), as reflected in workplace legislation (6). In this study, we investigated the hypothesis that purinergic signaling contributes to cochlear adaptation to elevated sound levels and protection from overstimulation. A complementary report by Yan et al. (7) shows that a dominant-negative point mutation in the ATP-gated ion channel $P2X_2$ receptor subunit underlies the autosomal-dominant nonsyndromic progressive hearing loss locus DFNA41. This study included data using the $P2X_2$ receptor-encoding gene knockout (*P2RX2*-null) mouse model, which demonstrated that noise exposure over a significant fraction of the animals' life caused selective high-frequency hearing loss.

The $P2X_2$ receptor is abundantly expressed by cells lining the cochlear partition, including the sensory hair cells of the organ of Corti, Reissner's membrane epithelial cells, and spiral ganglion neurons (8–10). The cochlear partition maintains the positive endocochlear potential (EP; ~+100 mV) that, along with the negative membrane potential of the hair cells, provides the driving force for sound transduction (11). Both EP and the hair cell membrane potential are reduced by activation of $P2X_2$-like ATP-gated nonselective cation channels (12, 13). In the guinea pig cochlea, noise stress causes release of ATP into the K^+-rich endolymphatic compartment, where $P2X_2$ receptors are concentrated (14). Thus, a role for ATP regulation of cochlear

Author contributions: G.D.H., S.M.V., K.E.F., J.M.E.C., B.S.K., P.R.T., and A.F.R. designed research; G.D.H., R.M.-J., S.M.V., R.S.T., V.P., S.F.T., A.C.Y.W., K.E.F., J.M.E.C., Y.S., P.S., B.S.K., P.R.T., and A.F.R. performed research; G.D.H., B.S.K., D.A.C., P.R.T., and A.F.R. contributed new reagents/analytic tools; G.D.H., R.M.-J., S.M.V., R.S.T., V.P., S.F.T., A.C.Y.W., K.E.F., J.M.E.C., Y.S., P.S., B.S.K., D.A.C., P.R.T., and A.F.R. analyzed data; and G.D.H., S.M.V., K.E.F., J.M.E.C., B.S.K., D.A.C., P.R.T., and A.F.R. wrote the paper.

The authors declare no conflict of interest.

*This Direct Submission article had a prearranged editor.

Freely available online through the PNAS open access option.

[1]To whom correspondence should be addressed. E-mail: g.housley@unsw.edu.au.

[2]P.R.T. and A.F.R. contributed equally to this work.

This article contains supporting information online at www.pnas.org/lookup/suppl/doi:10.1073/pnas.1222295110/-/DCSupplemental.

www.pnas.org/cgi/doi/10.1073/pnas.1222295110

function via $P2X_2$ receptors is well-established at the cellular and tissue level, but analysis of the potential contribution of this pathway to the regulation of hearing has previously lacked an appropriate animal model. Here we provide evidence that as the sound floor is elevated, ATP is released into the cochlear partition, activating $P2X_2$ receptors, which reduces sound transduction and synaptic transmission from the hair cells. This purinergic regulation of hearing sensitivity was revealed by the absence of temporary threshold shift (TTS) in *P2RX2*-null mice. The mechanism is otoprotective, as *P2RX2*-null mice are highly vulnerable to noise-induced hearing loss with more extensive acoustic overstimulation.

Moderate Noise TTS Is $P2X_2$ Receptor-Dependent

Auditory brainstem response (ABR) thresholds to tone pips (4–32 kHz) were initially compared between *P2RX2*-null mice and background wild-type (WT) strain (C57BL/6J) mice at 6 mo of age. Baseline thresholds were comparable (Fig. S1). Remarkably, the *P2RX2*-null mice lacked the pronounced increase in threshold (loss of hearing sensitivity) to a moderately high, closed-field noise exposure [30 min; 85 decibel sound pressure level (dB SPL); 8–16 kHz band-pass noise] evident in the WT controls when measured using click and 16-kHz tone pip stimuli within ~30 min of the noise exposure (Fig. 1 *A* and *B*). The difference in mean thresholds post- versus prenoise in WT mice was highly significant ($P < 0.001$, ranked ANOVA with Holm–Sidak, all pairwise multiple comparisons; $n = 9$), whereas *P2RX2*-null mice thresholds were not affected by the noise exposure ($P > 0.05$; $n = 7$). TTS was calculated by subtracting the immediate postnoise threshold from the prenoise (baseline) threshold for each mouse. The difference between *P2RX2*-null and WT TTS was correspondingly highly significant ($P < 0.001$; WT TTS vs. *P2RX2*-null TTS: click, $P = 0.007$ and 16 kHz, $P = 0.002$). TTS in WT mice measured by click stimulus was 10.6 ± 1.4 dB ($P < 0.001$, single-sample *t* test) compared with 2.1 ± 0.9 dB ($P = 0.045$) in *P2RX2*-null mice; WT 16-kHz TTS was 15.6 ± 4.8 dB ($P = 0.012$) compared with 1.4 ± 2.6 dB ($P = 0.596$) in *P2RX2*-null mice.

Cubic ($2f_1$-f_2) distortion product otoacoustic emissions (DPOAEs) recorded alongside ABR testing (before noise and ~30 min after noise), were used to assess outer hair cell function and cochlear micromechanics before and after noise exposure in *P2RX2*-null and WT mice. In the 6-mo-old WT group, the 30-min 85-dB octave band noise exposure significantly elevated the thresholds of DPOAEs arising from primary tones about 16 kHz ($P = 0.009$, paired *t* test; 19.4 ± 4.3 dB prenoise; 37.5 ± 5.0 dB postnoise; $n = 8$; average threshold shift 18.1 ± 5.1 dB), whereas DPOAE thresholds in *P2RX2*-null mice were not affected by the noise exposure ($P = 1.000$, Wilcoxon signed-rank test; $n = 7$; 25.5 ± 4.2 dB prenoise, 33.6 ± 4.3 dB postnoise; average threshold shift 7.9 ± 2.6 dB) (Fig. S2). DPOAEs reflect the contribution of the outer hair cell-derived cochlear amplifier to hearing sensitivity and frequency selectivity (15), and these data indicate that noise-induced $P2X_2$ receptor activation inhibits outer hair cell electromotility and affects cochlear micromechanics. This suppression of the cochlear amplifier would contribute to the elevation in thresholds (TTS) evident from the ABR recordings in WT animals. To further evaluate this, we assessed the noise-induced (closed-field, 85 dB, 8–16 kHz octave band noise) modulation of the operating point of the cochlear amplifier by measuring the change in amplitude of the cubic DPOAE about 16 kHz using 60-dB primary tones in WT mice ($n = 4$) compared with *P2RX2*-null ($n = 4$) littermates (3-mo-old). Both groups of mice had equivalent starting DPOAE amplitudes (WT 20.3 ± 1.8 dB SPL; *P2RX2*-null 19.7 ± 0.8 dB SPL; $P = 0.231$, *t* test). However, following 1–2.5 min of noise, *P2RX2*-null mice exhibited significantly less reduction in DPOAE amplitude than WT mice ($P < 0.05$; two-way repeated-measures ranked ANOVA; Fig. S3). The reduction in DPOAE amplitude changed from −34.5 ± 1.6 dB to −28.5 ± 2.8 dB over 45 min in WT mice, compared with a recovery from −27.0 ± 2.9 dB to −19.8 ± 4.1 dB in *P2RX2*-null mice.

The time course for the development of the $P2X_2$ receptor-dependent TTS was determined by successive 16-kHz tone pip ABR threshold measurements after 10, 40, and 110 min of noise exposure (closed-field, 4–32 kHz noise band, 85 dB SPL). The study used *P2RX2*-null mice and strain-matched WT controls (9–12 wk of age; $n = 3$ for each group). The WT mice showed rapid development of TTS (Fig. 2*A* and Fig. S4), which was significantly greater than the minimal change in thresholds in the *P2RX2*-null mice over the 2-h study period ($P = 0.002$, two-way ANOVA). ABR thresholds during noise exposure were subtracted from baseline threshold values prenoise ($t0$) to provide the TTS for each mouse. These data were fitted to a single exponential growth function [$f = 17.8 \times (1 - \exp[-0.0514 \times T_{(min)}])$; $R^2 = 0.942$] to yield a time constant of ~20 min for the development of TTS, with an asymptote of ~18 dB (Fig. 2*A*). In contrast, *P2RX2*-null mice had minimal TTS, with an ~6 dB asymptote [$P < 0.001$, two-way ANOVA versus WT group; *P2RX2*-null best fit: $f = 6.035 \times (1 - \exp[-0.0352 \times T_{(min)}])$; $R^2 = 0.988$].

The time course for recovery from $P2X_2$ receptor-dependent TTS was determined by measuring the ABR thresholds in WT, heterozygous [$P2RX2^{(+/-)}$], and homozygous knockout (*P2RX2*-null) littermates (8–12 wk; $n = 6$ per group) after 30 min of broadband noise (~TTS asymptote) (closed-field, 4–32 kHz, 85 dB SPL). The starting level of TTS (time 0; Fig. 2*B*) in the WT mice was 15.4 ± 2.2 dB, which was not significantly different from the TTS in the heterozygous $P2RX2^{(+/-)}$ mice (17.5 ± 3.8 dB; $P = 0.929$, one-way ANOVA with Holm–Sidak pairwise comparison). Predictably, *P2RX2*-null mice had no significant threshold shift (1.7 ± 0.8 dB; $P = 0.102$, one-sample *t* test). The difference between the *P2RX2*-null group and either WT or $P2RX2^{(+/-)}$ mice was highly significant ($P < 0.001$). These data indicate haplosufficiency in the development of $P2X_2$ receptor-dependent TTS. The ABR input/output functions were determined pre- and postnoise for the WT and *P2RX2*-null mice based on the amplitude of the p1-n1 wave (Fig. S5). These data indicate a significant noise-induced reduction in the gain of sound transduction in WT mice ($P < 0.001$, two-way ranked ANOVA) but not in *P2RX2*-null mice. There was no significant difference between the growth functions for the WT and *P2RX2*-null mice before noise. ABR thresholds were remeasured at 8, 24, and 96 h postnoise. The recovery of the threshold shift in WT mice had a time constant of 12.3 h [single exponential decay best fit; $f = 1.70 + 13.44 \times \exp(-0.0814 \times T_{(h)})$; $R^2 = 0.98$]. The recovery from TTS in the $P2RX2^{(+/-)}$ mice mapped to the WT recovery time course. These data indicate that 30 min of noise activation of $P2X_2$ receptor signaling (in WT mice) instigates a prolonged reduction in hearing sensitivity that takes more than 24 h to fully resolve.

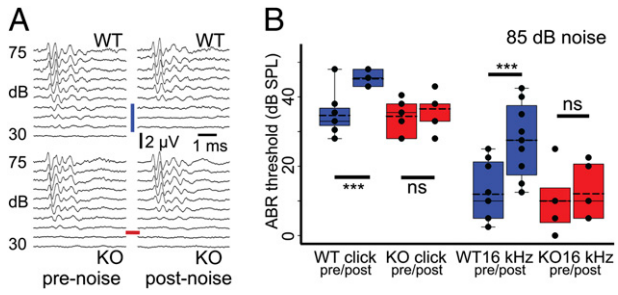

Fig. 1. *P2RX2*-null mice (KO) lacked TTS in response to moderate-intensity noise evident in WT controls. (*A*) Examples of ABR traces (10-ms duration) for click stimuli before and after 30-min noise (85 dB, closed-field). The threshold in the WT mouse increased from 32.5 dB to 45 dB (blue bar), whereas the *P2RX2*-null mouse threshold remained unchanged (red bar). (*B*) Box plots with data overlay showing the pre- and postnoise thresholds assessed using click and 16-kHz tone pip stimuli (***$P < 0.001$; ns, $P > 0.05$; $n = 9$ WT; $n = 7$ KO). Tests were within ~30 min postnoise exposure. Dashed lines show the means.

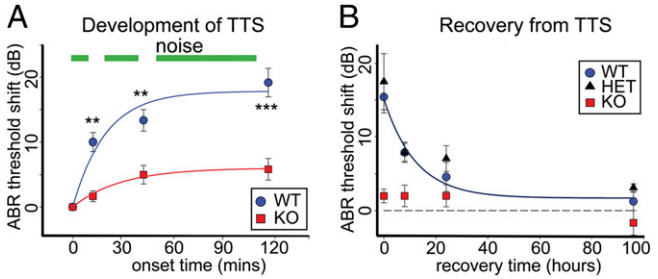

Fig. 2. TTS development and recovery. (*A*) Development of TTS was determined using 16-kHz ABR threshold measurements by briefly interrupting sustained noise (85 dB, 4–32 kHz, closed-field; K/X/A anesthesia); knockout (*P2RX2*-null) ($n = 3$) mice; wild-type ($n = 3$) age- and strain-matched control mice. Single exponential curve fits for TTS growth; time constant 19.5 min WT; 28.4 min KO. $P < 0.001$ KO vs. WT; $^{**}P = 0.003$, $^{***}P < 0.001$, two-way ANOVA, Holm–Sidak pairwise comparison. (*B*) Recovery of TTS in WT, HET [*P2RX2*$(^{+/-})$], and KO littermate mice using broadband noise (4–32 kHz, 30 min, closed-field; $n = 6$ each group). ABR (16-kHz) threshold measurements. $P < 0.001$ for KO vs. WT or HET, two-way ANOVA. TTS recovery time constant for WT or HET was 12.3 h.

P2RX2-Null Mice Have Greater Hearing Loss in High-Level Noise

We titrated the noise level to determine the contribution of cochlear $P2X_2$ receptor signaling to TTS and permanent threshold shift (PTS) at higher sound levels, levels that would be expected to induce more extensive TTS, but no PTS, in WT mice. Noise at 95 dB SPL for 30 min (8–16 kHz octave band, closed-field) caused substantial immediate threshold shifts in strain-matched WT mice ($n = 11$) (≥45 dB from 16 kHz) as well as *P2RX2*-null mice ($n = 11$) (10- to 13-wk-old) (Fig. 3*A*). Thus, $P2X_2$ receptor-dependent TTS was overshadowed by additional components at this noise level (no significant difference between genotypes, $P = 0.206$, two-way ANOVA, 4–24 kHz). Reassessment of ABR in both groups of mice 2 wk later indicated that the threshold shifts measured immediately after noise across the test frequencies in the WT mice were all TTS, whereas in the *P2RX2*-null mice there was a substantial (~20 dB) PTS at the highest frequency tested (24 kHz) ($P < 0.001$, one-sample t test). This transfer of the impact of loud sound to higher-frequency transducing regions of the cochlea is consistent with the well-established half-octave shift in the frequency of maximum loss that reflects the underlying cochlear amplifier energy delivery (16). This PTS was associated with a significantly greater immediate DPOAE threshold shift in *P2RX2*-null mice compared with WT (Fig. S6; $P = 0.026$, 16–28 kHz, two-way ANOVA), suggesting that in the absence of $P2X_2$ receptor activation at this high noise level, outer hair cells located basal to the tonotopic place for the noise band are overdriven.

The effects of sound levels that would be expected to induce PTS in WT mice were then assessed using open-field noise (2 h, 100 dB SPL, 8–16 kHz band-pass noise) in 3-mo-old *P2RX2*-null mice and strain-matched WT controls. Baseline ABR thresholds (click and tone pip stimuli) were again equivalent in *P2RX2*-null and WT mice before noise exposure. However, PTS assessed 2 wks after noise exposure was substantially and significantly higher in *P2RX2*-null mice. For click stimuli (Fig. 3*B*), the PTS in the *P2RX2*-null group was 18 dB greater than that of the WT controls ($P = 0.026$, Mann–Whitney rank-sum test; $n = 9$ *P2RX2*-null; $n = 8$ WT). Similarly, PTS at or above the frequency of the octave band noise was substantially (up to 32 dB) greater than that of the WT ($P < 0.001$, two-way ANOVA, Holm–Sidak pairwise comparison; Fig. 3*B*).

Histological analysis of the cochlear tissue from these 100 dB SPL noise-exposed mice at 6 wks postnoise, using toluidine blue-stained thin sections following resin embedding, indicated that there was significant ($P = 0.008$, two-tailed unpaired t test) atrophy of the spiral ganglion neurons in *P2RX2*-null mice (Fig. 3*C* and Fig. S7 *A*, *B*, and *E*). Somata size in the midcochlear region decreased from 118.9 ± 3.6 μm^2 (from averages of five WT cochleae) to 95.2 ± 5.8 μm^2 (from averages of four *P2RX2*-null cochleae) (95–162 neurons measured per cochlea). There was, however, no significant difference in neuron density (WT 32.9 ± 2.5, *P2RX2*-null 37.6 ± 5.6 neurons/10,000 μm^2; $P = 0.442$) that would indicate neuronal loss (Fig. S7*E*). Examination of phalloidin fluorescence-labeled whole-mounts from the 100-dB SPL, 2-h, open-field study showed that the inner and outer hair cell counts of WT and *P2RX2*-null mice were comparable, with no apparent bias in hair cell condition despite the considerable difference in PTS (Fig. S7 *C* and *D*). These observed histological changes are consistent with PTS arising from neural rather than hair cell injury. To further assess this possibility, we demonstrated in separate experiments using 100 dB SPL closed-field noise (1 h, 4–32 kHz) that *P2RX2*-null mice with PTS showed a considerable impact of noise on the inner hair cell type-I spiral ganglion synapse structure. The noise-induced changes at the hair cell–afferent fiber nexus included reduction in the number of C-terminal binding protein 2 (CtBP2)-immunolabeled ribbon synapses at the inner hair cells of the noise-treated versus untreated cochleae ($P = 0.015$, paired t test) from the same mice [Fig. 3*D*; mean 10.3 ± 1.0 puncta per inner hair cell (noise) vs. 17.5 ± 2.3 (control cochleae); counts from eight sequential optical sections at 1-μm spacing ($n = 4$)]. This was associated with attrition of peripheral afferent neurites projecting through the habenula perforata to form the inner spiral

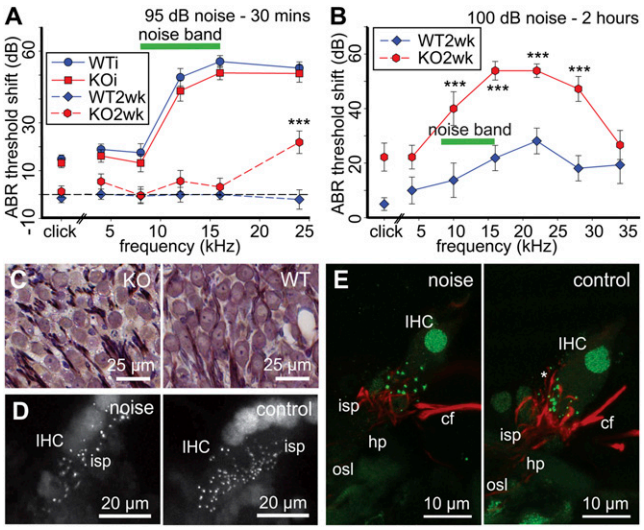

Fig. 3. Extreme levels of noise caused greater PTS in *P2RX2*-null mice (KO). (*A*) ABR thresholds in *P2RX2*-null mice increased to those of WT mice (age- and strain-matched control), measured immediately (WTi, KOi) following 95-dB noise (8–16 kHz, 30 min, closed-field, K/X/A anesthesia). In WT mice ($n = 8$), this was TTS, as the thresholds fully recovered by 2 wk (WT2wk), whereas PTS was evident ($^{***}P < 0.001$) at 24 kHz in *P2RX2*-null mice ($n = 9$). (*B*) *P2RX2*-null mice showed substantial PTS following exposure to longer-duration 100-dB noise (8–16 kHz, 2 h, awake, open-field). Click PTS and tone pip ABR threshold shifts, $^{***}P < 0.001$. (*C*) Toluidine blue-stained thin sections of the spiral ganglion from the PTS *P2RX2*-null and WT control groups from *B*, showing atrophy of the neuron somata in *P2RX2*-null cochlea. (*D*) Reduced density of inner hair cell ribbon synapses (CtBP2 immunofluorescence) evident in the noise-treated cochlear tissue (100 dB, 1 h, 4–32 kHz) compared with the control cochlea (no noise) from the same *P2RX2*-null mouse (PTS, ~50 dB at 16 kHz). Reconstruction of 50-μm cryosections. (*E*) Reconstruction of the afferent neurite innervation (neurofilament 200 immunolabeling; red) of individual inner hair cells showing noise-induced reduction in the density of terminals. Control is from the contralateral (untreated) cochlea (equivalent midbasal region) from the same *P2RX2*-null mouse. cf, crossing fibers (efferent); hp, habenula perforata; IHC, inner hair cell; isp, inner spiral plexus; osl, osseous spiral lamina. The asterisk highlights normal neurite projections juxtaposed to the ribbon synapses (CtBP2 immunofluorescence; green) on the basolateral membrane of a control IHC.

plexus that envelops the base of the inner hair cells (neurofilament 200 immunolabeling; Fig. 3*E*). These data indicate a direct effect on hair cell synapses and neurons, likely via glutamatergic excitotoxicity (17). Data from control experiments, where wild-type mice were exposed to a noise level known not to produce PTS (95 dB noise, 8–16 kHz, closed-field, 30 min, as for Fig. 2*A*), showed that there was no difference in CtBP2 puncta per inner hair cell between left (untreated) versus right (noise-exposed) cochleae (noise: 17.0 ± 2.6; no noise: 19.0 ± 2.7; $P = 0.558$, paired t test; $n = 5$). These data indicate that unlike the noise-exposed cochleae susceptible to PTS due to loss of $P2X_2$ receptor signaling, decreased synaptic density does not occur in wild-type mice exposed to loud noise insufficient to drive PTS with $P2X_2$ receptor signaling in place. Noise-exposed wild-type mice with PTS are known to exhibit decreased CtBP2 labeling (18).

Sites of Action

Immunofluorescence confirmed the cochlear partition as the principal site of $P2X_2$ receptor expression in WT mice (Fig. 4*A*, Fig. S8, and Movie S1). $P2X_2$ receptor immunolabeling included all of the cells lining the endolymphatic compartment with the exception of the marginal cells of the stria vascularis. In contrast, $P2X_2$ receptor immunolabeling in the spiral ganglion was minimal. This mouse cochlear $P2X_2$ receptor distribution matched the $P2X_2$ receptor mRNA transcript expression in the rat cochlea detected by in situ hybridization (8). Specificity of the immunolabeling was confirmed by the absence of signal in *P2RX2*-null cochlear tissue.

The cellular physiology of the cochlear partition was investigated by patch-clamp analysis of Reissner's membrane epithelial cells as well as the inner and outer hair cells. These cell types have previously been shown to have substantial ATP-gated nonselective cation conductances localized to the endolymphatic surface in guinea pig (9, 10, 19, 20), rat (21), and mouse (22). In no case was an ATP-activated inward current recorded from *P2RX2*-null Reissner's membrane epithelial cells ($n = 30$), inner hair cells ($n = 15$), or outer hair cells ($n = 6$). In contrast, in WT tissue, Reissner's membrane epithelial cells had a mean ATP-activated inward current of −2.06 ± 0.17 nA; $n = 63/63$ cells responded; outer hair cells had a mean inward current of −312 ± 78 pA; $n = 7/7$ cells; and inner hair cells had a mean inward current of −304 ± 210 pA (3/16 cells responded to ATP) (Fig. 4 *B* and *C*). Of note was the approximately sevenfold larger ATP-gated inward currents in the Reissner's membrane cells compared with the hair cells. The substantial Reissner's membrane ATP-activated conductance indicates that this element of the cochlear partition would contribute significantly to the overall ATP-induced reduction in cochlear partition resistance (CoPR) evident when ATP is introduced into the endolymphatic compartment (*Discussion*). There were no significant differences in resting membrane potential, measured at zero current, or variations in voltage-dependent conductance, between *P2RX2*-null and WT for any of the cell types (Table S1) to indicate that the absence of the $P2X_2$ receptor had any bearing on the properties of the cells other than the loss of the capability for ATP-gated inward current.

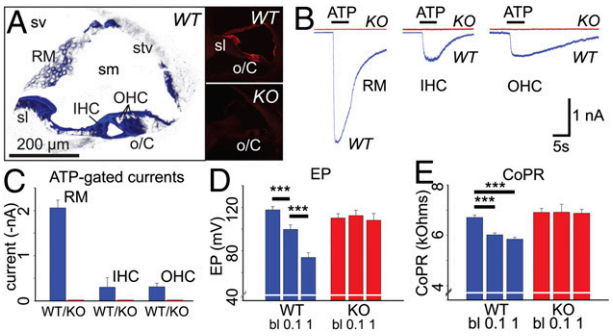

Fig. 4. Localization of $P2X_2$ receptor expression in the cochlear partition and assessment of ATP-gated conductances. (*A*) $P2X_2$ receptor immunofluorescence. Note the strong signal in WT cochlea, on Reissner's membrane epithelial cells (RM), spiral limbus (sl), and organ of Corti (o/C), including the inner and outer hair cells (IHCs and OHCs, respectively) (pseudocolored projection of confocal image stack of immunofluorescence from a 50-μm cryosection; 3-mo-old mouse). sm, scala media; stv, stria vascularis; sv, scala vestibuli. (*Right*) Unprocessed immunofluorescence images for WT and *P2RX2*-null tissue (KO). (*B*) Examples of whole-cell voltage-clamp recordings from RM, IHC, and OHC. Records from cells isolated from KO and WT tissue are overlaid. Bars indicate the 5-s applications of 100 μM ATP at a holding potential of −60 mV. (*C*) Average ATP-induced current responses from RM, IHC, and OHC from WT cochleae, compared with no responses in cells from *P2RX2*-null mice. (*D*) Microinjection of ATP (0.1 and 1 mM, 10 nL) into scala media produced a dose-dependent reduction in EP in WT mice that was absent in *P2RX2*-null mice. bl, baseline. (*E*) Associated dose-dependent reduction in CoPR produced by ATP in WT mice. There was no change in CoPR in *P2RX2*-null mice. ***$P < 0.001$.

The effect of ATP injection into the endolymphatic compartment on the EP and CoPR was assessed in vivo to establish whether additional ATP-activated conductance remained in the absence of $P2X_2$ expression in the cochlear partition cell types tested by patch-clamp. As established in the guinea pig model (12), microinjection of ATP into scala media in WT mice produced a significant fall in EP and a corresponding reduction in CoPR (Fig. 4 *D* and *E*). The EP directly impacts on the driving force for sound transduction (11). *P2RX2*-null mice failed to show any change in EP or CoPR when ATP [100 μM ($n = 5$) or 1 mM ($n = 7$)] ($n = 12$ baseline measurements) was injected (10 nL) into scala media ($P = 0.009$, two-way ranked ANOVA compared with WT). WT mice showed a dose-dependent reduction in EP [15% at 100 μM ATP ($P < 0.001$, one-way ranked ANOVA [$n = 13$] vs. baseline [$n = 25$]) and 37% at 1 mM ATP ($P = 0.001$ vs. 100 μM ATP, paired t test; $n = 12$)]. The baseline EP was similar in both groups (118.0 ± 3.0 mV WT, 110.0 ± 4.0 mV *P2RX2*-null; $P = 0.154$, unpaired t test). The ATP-induced fall in EP in WT mice reflects the capacity of the cells lining scala media to shunt K^+ across the cochlear partition via the ATP-gated nonselective cation channels (12). The increase in conductance in these cells is evident in the associated dose-dependent reduction in CoPR in the WT mice ($P < 0.001$ baseline vs. 100 μM and 1 mM ATP; one-way ANOVA). There was no change in CoPR with ATP injection in *P2RX2*-null mice ($P < 0.001$ compared with WT, two-way ANOVA), whereas baseline resistance was not significantly different from that of the WT mice (WT 6.71 ± 0.10 kΩ, *P2RX2*-null 6.91 ± 0.16 kΩ; $P = 0.236$). Given that the endolymph volume of the mouse cochlea is ~0.2 μL (23), we estimate ~5–50 μM ATP concentrations arising from the 10-nL injections, which approaches the EC_{50} for ATP-gated ion channels assembled from $P2X_2$ receptor subunits (24).

These data indicate that in *P2RX2*-null mice there is no detectable compensation due to up-regulation of other P2X receptor subtypes (indicating homomeric $P2X_2$ receptor subunit assembly of the ATP-gated ion channels) across the range of epithelial cells shown to express $P2X_2$ receptors (Fig. 4*A* and Fig. S8). In addition, these data, and the normal hearing function of *P2RX2*-null mice in the absence of noise stimulation, make it unlikely that critical molecular pathways supporting sound transduction and synaptic transmission have been affected by the knockout of the *P2RX2* gene. Noise-induced ATP release would therefore be unable to invoke cation conductance in the sensory epithelium and other elements of the cochlear partition that control sound transduction in *P2RX2*-null mice.

Discussion

P2RX2-null mice failed to exhibit the initial 15 dB of threshold shift produced when sound level was elevated. WT mice developed this TTS with a 20-min time constant. The impact of moderate noise on cochlear function was also reflected in the substantial decrease in suprathreshold ABR amplitude in WT mice compared with the preserved gain of the ABR input/output

function of *P2RX2*-null mice. Recovery from the $P2X_2$ receptor-dependent TTS had a 12-h time constant, which is similar to the situation with human subjects exposed to TTS-level sound (25). In the absence of $P2X_2$ receptor signaling, the cochlea was more vulnerable to damage from excessive noise, evident as PTS in the *P2RX2*-null mice at the higher presented sound levels. Given that perceived loudness halves every 10 dB and sound intensity halves every 3 dB, this $P2X_2$ receptor-dependent hearing modulation provides a substantial downward adjustment of the operational point of sound transduction and auditory neurotransmission in the cochlea at high sustained sound levels. These characteristics provide strong support for the postulate that sound-induced activation of $P2X_2$ receptors in the cochlea underlies a local autocrine/paracrine purinergic adaptation mechanism that sustains the upper physiological range of hearing.

Although it is appreciated that TTS (reversible within hours to days) and PTS are not a continuum of cochlear pathophysiology due to acoustic overstimulation, noise-induced threshold changes are multifactorial, as revealed by histological, physiological, proteomic, and transcriptional studies of the cellular and molecular responses of the cochlea to loud sound (e.g., 17, 25–29). The mechanisms underlying TTS have remained speculative, although studies suggest that oxidative stress at the inner hair cell afferent synapse is significant (30). Even low-level noise stress (producing TTS) can have long-term downstream consequences for hearing—evident in earlier development of hearing loss with aging (31).

The identification that purinergic signaling drives TTS as the background sound level rises is key evidence that such TTS is fundamentally adaptive. Neural regulation via the olivocochlear efferent innervation to the outer hair cells can certainly protect the cochlea from noise-induced hearing loss (5, 32), but the kinetics for efferent regulation of cochlear function, such as contralateral suppression via the medial olivocochlear bundle, have fast time constants (4) inconsistent with TTS. The most parsimonious explanation arising from our study is that $P2X_2$ receptor activation, as a result of noise-induced ATP release in the cochlea, represents the primary upstream signaling element causing the dominant component of TTS at moderate sustained noise levels, and this reflects physiological adaptation to noise rather than an injury response. Certainly, the preservation of hearing sensitivity in the face of sustained 85-dB noise exposure in *P2RX2*-null mice attests to the lack of immediate tissue damage as an underlying cause of the TTS in WT mice at this sound level. This adaptation process would enable cochlear hair cells to encode the upper component of the physiological hearing range in background noise without damage. A potential caveat to our results is that the *P2RX2*-null mice lacked $P2X_2$ receptor expression in the cochlea from early development. However, underlying hearing physiology was normal (Fig. S1; see also ref. 7). Older *P2RX2*-null mice do exhibit selective hearing loss, evident as exacerbated presbycusis compared with wild-type controls at 18 mo of age raised in the quiet (7).

The mechanism of the $P2X_2$ receptor-dependent reduction in hearing sensitivity surely involves the movement of cations (including a high Ca^{2+} conductance) through $P2X_2$ receptor homomeric ATP-gated channels (24). At a tissue level, it has been shown that release of ATP into the endolymphatic compartment causes a rapid shunt of K^+ entering the ATP-gated ion channels (12) (confirmed here as exclusively $P2X_2$ receptor-mediated), which, via the associated fall in EP, and parallel depolarization of the hair cells, would contribute to regulation of sound transduction. However, extracellular ATP is rapidly hydrolyzed by ecto-ATPases (33). Because TTS arising from 30 min of 85-dB noise persisted for hours, well beyond the likely period of elevated extracellular ATP, a more sustained effect must underlie $P2X_2$ receptor-dependent TTS. A clue may be found in the observation that outer hair cell electromotility (reverse transduction) in WT mice was compromised with TTS (DPOAE threshold was elevated and DPOAE amplitude was suppressed; Figs. S2 and S3), alongside the increase in ABR threshold (decreased neural output). EP recovers rapidly after cessation of noise, and direct action of K^+ efflux is also unlikely to account for the TTS, as clearance of sound-induced K^+ buildup around the inner hair cells is too rapid (34). The hair cell transducer conductance (forward transduction) is relatively resistant to acoustic overstimulation, where, despite considerable increases in cochlear nerve thresholds (TTS), cochlear microphonic output (a population measure of outer hair cell receptor potential) is sustained (35). Based on reduced tuning of basilar membrane displacement associated with this TTS, it has been proposed that outer hair cell reverse transduction (rather than forward transduction) was affected (35). Ca^{2+}-mediated adaptation affecting outer hair cell electromotility (36) and supporting cell micromechanical compliance, as well as Ca^{2+}-regulated adaptation at the inner hair cell ribbon synapse (37, 38), are all processes likely to be impacted by the distributed cochlear $P2X_2$ receptor signaling.

Our findings generate an apparent paradox in that moderate noise fails to affect hearing in *P2RX2*-null mice (speaking to the robust nature of forward and reverse transduction without $P2X_2$ receptor-dependent adaptation) but loud noise causes enhanced PTS in these animals. This dichotomy in sensitivity to noise in *P2RX2*-null mice can be reconciled if the TTS-level adaptation arising from noise-activated $P2X_2$ receptor signaling protects transduction and transmission at the hair cells from excessive acoustic stimulation, whereas PTS, focused at the inner hair cell–spiral ganglion synapse, arises from overdrive of these processes in the absence of this purinergic adaptation mechanism. Noise-induced glutamate excitotoxicity is well-established in the cochlea (17, 27), and is correlated with loss of the spiral ganglion punctate synapses, atrophy of the neuron soma, and, presynaptically, loss and dislocation of the CtBP2-labeled ribbon synapses (18). All of these characteristics match the cochlear structural profile of *P2RX2*-null mice with PTS.

The identification of the $P2X_2$ receptor as a key element of hearing adaptation suggests that factors that compromise this process, such as age-related muting of $P2X_2$ receptor-dependent regulation of cochlear partition conductance (39), or polymorphisms within the *P2RX2* gene, contribute to variation in susceptibility to noise-induced hearing loss in society. Indeed, the present study clearly complements our recent report (7), which showed that the absence of cochlear $P2X_2$ receptor signaling in two Chinese families, attributable to a dominant-negative mutation P2RX2 c.178G>T (p.V60L), removed intrinsic purinergic otoprotection from the hearing organ and precipitated the DFNA41 autosomal-dominant progressive hearing loss. DFNA41 subjects with a history of noise exposure had exacerbated high-frequency hearing loss, an effect that was modeled in *P2RX2*-null mice exposed to long-term noise exposure. In identifying a key molecular element of hearing adaptation to sustained noise stressors, the present study provides a timely reinforcement of the consequence of exceeding the capacity of our hearing organ to cope with loud sound. These experiments open a path for analysis of the mechanisms for sound-evoked ATP release into the cochlear tissues associated with this $P2X_2$ receptor signaling, including potential contributions from P2Y receptors linked to ATP release (40), and cellular elements that sustain dynamic adaptation to changes in sound level over a lifetime.

Materials and Methods

Additional details of methodology are provided online in *SI Materials and Methods*.

***P2RX2*-null mouse model.** This study used *P2RX2*-null mice (*B6.129-P2rx2*^{tm1Ckn}*/J*), which have previously enabled elucidation of the role of $P2X_2$ receptors in a range of sensory modalities, including pain sensation and urinary bladder reflexes (41). These mice, and strain-matched C57BL/6J WT mice, were obtained as breeding stock from The Jackson Laboratory. *P2RX2*-null mice and WT littermates were generated using heterozygous (*P2RX2*$^{(+/-)}$) breeding pairs derived from crossing these lines. The C57BL/6J strain is commonly used for transgenic mouse line development and has been extensively studied for hearing function, including the identification of a mutation in the *Cdh23* gene that impacts age-related hearing loss (42). The studies were approved by the University of Auckland Animal Ethics Committee, the local animal subjects committee of the San Diego Veterans

Affairs Healthcare System, and the University of New South Wales Animal Care and Ethics Committee. The mice were maintained in individually ventilated cages (VentiRack; BioZone).

ABR and DPOAE. Sound levels are presented as dB sound pressure level (SPL). Click and puretone ABR thresholds and cubic DPOAEs ($2f_1$-f_2) were measured under ketamine/xylazine/acepromazine (K/X/A) anesthesia as previously described (43). $P2X_2$ receptor-dependent TTS was produced using 85 dB SPL noise (8–16 kHz or 4–32 kHz), delivered via the ear probe (closed-field). PTS was generated in conscious mice using 2-h 100-dB SPL open-field broadband noise (8–16 kHz band-pass), or under K/X/A anesthesia (4–32 kHz, 100 dB SPL, 1 h, closed-field).

Endocochlear Potential and Cochlear Partition Resistance. EP and CoPR measurements were made under urethane anesthesia as previously described (12), with the minor modification of a 500-ms 1-μA current pulse at 50% duty cycle.

Cellular Physiology. Whole-cell patch-clamp recordings from Reissner's membrane epithelial cells and hair cells were made in situ as previously described (22). Cells were voltage-clamped at −60 mV and ATP pressure-applied to the cells via a glass micropipette.

Immunolabeling. Immunofluorescence imaging of $P2X_2$ receptor expression used an anti-$P2X_2$ receptor polyclonal antiserum (Alomone). CtBP2 immunolabeling of the hair cell ribbon synapses used an anti-CtBP2 antisera (BD Biosciences). Neurofilament 200 immunolabeling of spiral ganglion neurite projections to the hair cell synapses used an anti-neurofilament 200 antibody (Sigma). After mounting, the immunolabeling was imaged using a Zeiss 710 confocal microscope.

Data Analysis. Parametric and nonparametric data comparisons were performed using two-way ANOVA, Student *t* tests, Mann–Whitney rank-sum tests, and Wilcoxon signed-rank tests after assessment of normality and variance (SigmaPlot version 11; Systat Software). Threshold for significance $\alpha = 0.05$, with Holm–Sidak all pairwise multiple comparison, where appropriate. Data are presented with SE (SEM).

ACKNOWLEDGMENTS. We thank Kwang Pak, Eduardo Chavez, Preet Singh, Myungseo Ko, and Jeremy Pinyon for assistance with these studies. This work was supported by National Health and Medical Research Council of Australia Grant 630618 (to G.D.H. and A.F.R.); the Health Research Council of New Zealand and Deafness Research Foundation of New Zealand (G.D.H., S.M.V., and P.R.T.); the Marsden Fund (Royal Society of New Zealand) (G.D.H.); and Veterans Affairs Research Service and National Institutes of Health Grant DC000139 (to A.F.R.).

1. Elliott SJ, Shera CA (2012) The cochlea as a smart structure. *Smart Mater Struct* 21(6): 64001.
2. Gates GA, Schmid P, Kujawa SG, Nam B, D'Agostino R (2000) Longitudinal threshold changes in older men with audiometric notches. *Hear Res* 141(1-2):220–228.
3. Mukerji S, Windsor AM, Lee DJ (2010) Auditory brainstem circuits that mediate the middle ear muscle reflex. *Trends Amplif* 14(3):170–191.
4. Maison SF, et al. (2012) Contralateral-noise effects on cochlear responses in anesthetized mice are dominated by feedback from an unknown pathway. *J Neurophysiol* 108(2):491–500.
5. Attanasio G, et al. (1999) Protective effect of the cochlear efferent system during noise exposure. *Ann N Y Acad Sci* 884:361–367.
6. Secretary of State UK (2005) The Control of Noise at Work Regulations, Health and Safety (Secretary of State UK), Statutory Instruments no. 1643. Available at www.legislation.gov.uk/uksi/2005/1643/contents/made.
7. Yan D, et al. (2013) Mutation of the ATP-gated $P2X_s$ receptor leads to progressive hearing loss and increased susceptibility to noise. *Proc Natl Acad Sci USA* 110(6): 2228–2233.
8. Housley GD, Luo L, Ryan AF (1998) Localization of mRNA encoding the $P2X_2$ receptor subunit of the adenosine 5′-triphosphate-gated ion channel in the adult and developing rat inner ear by in situ hybridization. *J Comp Neurol* 393(4):403–414.
9. King M, Housley GD, Raybould NP, Greenwood D, Salih SG (1998) Expression of ATP-gated ion channels by Reissner's membrane epithelial cells. *Neuroreport* 9(11): 2467–2474.
10. Housley GD, et al. (1999) Expression of the $P2X_2$ receptor subunit of the ATP-gated ion channel in the cochlea: Implications for sound transduction and auditory neurotransmission. *J Neurosci* 19(19):8377–8388.
11. Nin F, et al. (2008) The endocochlear potential depends on two K^+ diffusion potentials and an electrical barrier in the stria vascularis of the inner ear. *Proc Natl Acad Sci USA* 105(5):1751–1756.
12. Thorne PR, Muñoz DJ, Housley GD (2004) Purinergic modulation of cochlear partition resistance and its effect on the endocochlear potential in the guinea pig. *J Assoc Res Otolaryngol* 5(1):58–65.
13. Ashmore JF, Ohmori H (1990) Control of intracellular calcium by ATP in isolated outer hair cells of the guinea-pig cochlea. *J Physiol* 428:109–131.
14. Muñoz DJ, Kendrick IS, Rassam M, Thorne PR (2001) Vesicular storage of adenosine triphosphate in the guinea-pig cochlear lateral wall and concentrations of ATP in the endolymph during sound exposure and hypoxia. *Acta Otolaryngol* 121(1):10–15.
15. Janssen T, Niedermeyer HP, Arnold W (2006) Diagnostics of the cochlear amplifier by means of distortion product otoacoustic emissions. *ORL J Otorhinolaryngol Relat Spec* 68(6):334–339.
16. Mellado Lagarde MM, Drexl M, Lukashkin AN, Zuo J, Russell IJ (2008) Prestin's role in cochlear frequency tuning and transmission of mechanical responses to neural excitation. *Curr Biol* 18(3):200–202.
17. Puel JL, Ruel J, Gervais d'Aldin C, Pujol R (1998) Excitotoxicity and repair of cochlear synapses after noise-trauma induced hearing loss. *Neuroreport* 9(9):2109–2114.
18. Kujawa SG, Liberman MC (2009) Adding insult to injury: Cochlear nerve degeneration after "temporary" noise-induced hearing loss. *J Neurosci* 29(45):14077–14085.
19. Housley GD, Greenwood D, Ashmore JF (1992) Localization of cholinergic and purinergic receptors on outer hair cells isolated from the guinea-pig cochlea. *Proc Biol Sci* 249(1326):265–273.
20. Housley GD, Raybould NP, Thorne PR (1998) Fluorescence imaging of Na^+ influx via P2X receptors in cochlear hair cells. *Hear Res* 119(1-2):1–13.
21. Wang JC, et al. (2003) Noise induces up-regulation of $P2X_2$ receptor subunit of ATP-gated ion channels in the rat cochlea. *Neuroreport* 14(6):817–823.
22. Järlebark LE, Housley GD, Raybould NP, Vlajkovic S, Thorne PR (2002) ATP-gated ion channels assembled from $P2X_2$ receptor subunits in the mouse cochlea. *Neuroreport* 13(15):1979–1984.
23. Thorne M, et al. (1999) Cochlear fluid space dimensions for six species derived from reconstructions of three-dimensional magnetic resonance images. *Laryngoscope* 109(10):1661–1668.
24. Kanjhan R, Raybould NP, Jagger DJ, Greenwood D, Housley GD (2003) Allosteric modulation of native cochlear P2X receptors: Insights from comparison with recombinant $P2X_2$ receptors. *Audiol Neurootol* 8(3):115–128.
25. Patuzzi R (1998) Exponential onset and recovery of temporary threshold shift after loud sound: Evidence for long-term inactivation of mechano-electrical transduction channels. *Hear Res* 125(1-2):17–38.
26. Taggart RT, et al. (2001) Gene expression changes in chinchilla cochlea from noise-induced temporary threshold shift. *Noise Health* 3(11):1–18.
27. Wang Y, Hirose K, Liberman MC (2002) Dynamics of noise-induced cellular injury and repair in the mouse cochlea. *J Assoc Res Otolaryngol* 3(3):248–268.
28. Selivanova O, Brieger J, Heinrich UR, Mann W (2007) Akt and c-Jun N-terminal kinase are regulated in response to moderate noise exposure in the cochlea of guinea pigs. *ORL J Otorhinolaryngol Relat Spec* 69(5):277–282.
29. Yamashita D, Minami SB, Kanzaki S, Ogawa K, Miller JM (2008) Bcl-2 genes regulate noise-induced hearing loss. *J Neurosci Res* 86(4):920–928.
30. Yamasoba T, Pourbakht A, Sakamoto T, Suzuki M (2005) Ebselen prevents noise-induced excitotoxicity and temporary threshold shift. *Neurosci Lett* 380(3):234–238.
31. Kujawa SG, Liberman MC (2006) Acceleration of age-related hearing loss by early noise exposure: Evidence of a misspent youth. *J Neurosci* 26(7):2115–2123.
32. Rajan R (1995) Involvement of cochlear efferent pathways in protective effects elicited with binaural loud sound exposure in cats. *J Neurophysiol* 74(2):582–597.
33. Vlajkovic SM, Thorne PR, Housley GD, Muñoz DJ, Kendrick IS (1998) Ecto-nucleotidases terminate purinergic signalling in the cochlear endolymphatic compartment. *Neuroreport* 9(7):1559–1565.
34. Johnstone BM, Patuzzi R, Syka J, Syková E (1989) Stimulus-related potassium changes in the organ of Corti of guinea-pig. *J Physiol* 408:77–92.
35. Fridberger A, Zheng J, Parthasarathi A, Ren T, Nuttall A (2002) Loud sound-induced changes in cochlear mechanics. *J Neurophysiol* 88(5):2341–2348.
36. Frolenkov GI, Mammano F, Belyantseva IA, Coling D, Kachar B (2000) Two distinct Ca^{2+}-dependent signaling pathways regulate the motor output of cochlear outer hair cells. *J Neurosci* 20(16):5940–5948.
37. Nouvian R, Beutner D, Parsons TD, Moser T (2006) Structure and function of the hair cell ribbon synapse. *J Membr Biol* 209(2-3):153–165.
38. Chen Z, Kujawa SG, Sewell WF (2007) Auditory sensitivity regulation via rapid changes in expression of surface AMPA receptors. *Nat Neurosci* 10(10):1238–1240.
39. Telang RS, et al. (2010) Reduced $P2x_2$ receptor-mediated regulation of endocochlear potential in the ageing mouse cochlea. *Purinergic Signal* 6(2):263–272.
40. Lahne M, Gale JE (2008) Damage-induced activation of $ERK_{1/2}$ in cochlear supporting cells is a hair cell death-promoting signal that depends on extracellular ATP and calcium. *J Neurosci* 28(19):4918–4928.
41. Cockayne DA, et al. (2005) $P2X_2$ knockout mice and $P2X_2/P2X_3$ double knockout mice reveal a role for the $P2X_2$ receptor subunit in mediating multiple sensory effects of ATP. *J Physiol* 567(Pt 2):621–639.
42. Noben-Trauth K, Zheng QY, Johnson KR (2003) Association of cadherin 23 with polygenic inheritance and genetic modification of sensorineural hearing loss. *Nat Genet* 35(1):21–23.
43. Cederholm JM, et al. (2012) Differential actions of isoflurane and ketamine-based anaesthetics on cochlear function in the mouse. *Hear Res* 292(1-2):71–79.